Computational Insights into Captopril's Inhibitory Potential Against MMP9 and LCN2 in Bladder Cancer: Implications for Therapeutic Application

Cancer Informatics
Volume 23: 1–13

DOI: 10.1177/11769351241276759

Sanjida Kabir Annana[1], Jannatul Ferdoush[2], Farzia Lamia[1], Ayan Roy[3], Pallab Kar[4], Monisha Nandi[5], Maliha Kabir[3] and Ayan Saha[3]

[1]Department of Genetic Engineering and Biotechnology, East West University, Dhaka, Bangladesh. [2]Department of Biology, Geology and Environmental Science, University of Tennessee at Chattanooga, Chattanooga, TN, USA. [3]Department of Bioinformatics and Biotechnology, Asian University for Women, Chattogram, Bangladesh. [4]Mailman School of Public Health, Columbia University, New York, NY, USA. [5]Department of Pharmacy, BGC Trust University Bangladesh, Chattogram, Bangladesh.

ABSTRACT

OBJECTIVES: Captopril is a commonly used therapeutic agent in the management of renovascular hypertension (high blood pressure), congestive heart failure, left ventricular dysfunction following myocardial infarction, and nephropathy. Captopril has been found to interact with proteins that are significantly associated with bladder cancer (BLCA), suggesting that it could be a potential medication for BLCA patients with concurrent hypertension.

METHODS: DrugBank 5.0 was utilized to identify the direct protein targets (DPTs) of captopril. STRING was used to analyze the multiple protein interactions. TNMPlot was used for comparing gene expression in normal, tumor, and metastatic tissue. Then, docking with target proteins was done using Autodock. Molecular dynamics simulations were applied for estimate the diffusion coefficients and mean-square displacements in materials.

RESULTS: Among all these proteins, *MMP9* is observed to be an overexpressed gene in BLCA and its increased expression is linked to reduced survival in patients. Our findings indicate that captopril effectively inhibits both the wild type and common mutated forms of *MMP9* in BLCA. Furthermore, the *LCN2* gene, which is also overexpressed in BLCA, interacts with captopril-associated proteins. The overexpression of *LCN2* is similarly associated with reduced survival in BLCA. Through molecular docking analysis, we have identified specific amino acid residues (Tyr179, Pro421, Tyr423, and Lys603) at the active pocket of MMP9, as well as Tyr78, Tyr106, Phe145, Lys147, and Lys156 at the active pocket of LCN2, with which captopril interacts. Thus, our data provide compelling evidence for the inhibitory potential of captopril against human proteins MMP9 and LCN2, both of which play crucial roles in BLCA.

CONCLUSION: These discoveries present promising prospects for conducting subsequent validation studies both in vitro and in vivo, with the aim of assessing the suitability of captopril for treating BLCA patients, irrespective of their hypertension status, who exhibit elevated levels of MMP9 and LCN2 expression.

KEYWORDS: Captopril, bladder cancer (BLCA), MMP9, hypertension, LCN2, inhibition, molecular dynamics simulation

RECEIVED: December 23, 2023. **ACCEPTED:** July 31, 2024.

TYPE: Original Research

FUNDING: The author(s) received no financial support for the research, authorship, and/or publication of this article.

DECLARATION OF CONFLICTING INTERESTS: The author(s) declared no potential conflicts of interest with respect to the research, authorship, and/or publication of this article.

CORRESPONDING AUTHOR: Ayan Saha, Department of Bioinformatics and Biotechnology; Asian University for Women, M. M. Ali Road, Chattogram 4000, Bangladesh. Email: ayan.saha.bd@gmail.com.

Highlights

- MMP9 overexpression in BLCA, linked to reduced survival, is effectively inhibited by captopril.
- Molecular docking identifies key amino acid residues for captopril interaction, suggesting potential therapeutic use for BLCA.
- Elevated LCN2 levels, associated with poor BLCA survival, also interact with captopril-related proteins.
- Captopril's inhibitory effects on both MMP9 and LCN2 hold promise for treating BLCA patients with hypertension.

Introduction

Captopril is commonly used in the treatment of renovascular hypertension, congestive heart failure, left ventricular dysfunction following myocardial infarction, and nephropathy. Captopril is an effective, competitive inhibitor of the angiotensin-converting enzyme (ACE), which transforms angiotensin I (ATI) into angiotensin II (ATII).[1] ATII is a strong vasoconstrictor hormone, that means it constricts the blood vessels, leading to an increase in blood pressure. Therefore, Captopril is used to treat high blood pressure by blocking the production of ATII. By blocking this hormone. Thus, captopril helps to relax blood vessels and reduce blood pressure. Captopril has been also shown to

have preventive benefits against organ damage brought on by hypertension (high blood pressure). According to 96 studies involving 1570 patients, captopril was found to be superior to placebo and equivalent to beta-blocker or diuretic in the treatment of hypertension.[2] Furthermore, it was found that Captopril prevents insulin-dependent diabetic nephropathy from worsening renal function.[3] Another study showed that patients on long-term captopril therapy may experience unexpected advantages from its antiangiogenic properties.[4] Thus, Captopril plays an important role in the treatment of hypertension.

Importantly, Hypertension has also been found to be associated with an increased risk of developing certain types of cancer and cancer-related mortality rates.[5] The association between hypertension and cancer diseases are multidimensional, and they have common risk factors such as smoking, diabetes mellitus, and obesity.[6] The prevalence of hypertension in patients with cancer was similar in the general adult population.[7] Research demonstrated that Captopril may have some anticancer properties. Notably, Captopril could be a promising option in the treatment of lung cancer.[8] It was found that Captopril could be used to prevent or reduce the severity of radiation-induced pulmonary toxicity in patients, radiation treatment for lung cancer.[9] Moreover, several studies in prostate cancer showed that captopril could inhibit the growth and proliferation of prostate cancer cells in vitro and in vivo.[10] Thus, Captopril medication may have a protective effect against the development of prostate cancer.[11]

In this study, we introduced an integrated analysis as an effective approach, which could analyze and prioritize candidate genes through the public databases. Firstly, we discovered direct protein targets (DPTs) of captopril in DrugBank 5.0. Subsequently, we analyzed the protein-protein interaction (PPI) network and signaling pathways of captopril DPTs. Refined analysis of KEGG (Kyoto Encyclopedia of Genes and Genomes) pathways showed that captopril is linked to various types of cancer, particularly Bladder cancer (BLCA). Another study also indicates that captopril can help maintain bladder structure.[12] Next, we identified 2 genes (*MMP2* and *MMP9*) as the most significant target genes of captopril in BLCA. Simultaneously, we analyzed the expression of these genes in BLCA, comparing them with normal samples, and examined the survival of BLCA patients associated with these genes. Finally, molecular docking and molecular simulation were employed to analyze the interaction pattern of captopril with the proteins associated with the poor survival of BLCA. Consequently, this study aims to elucidate the potential use of captopril in managing hypertension or heart failure in BLCA patients.

Material and Methods

Recognition for direct protein targets (DPTs) of captopril

DrugBank is a web-based database that contains detailed molecular data on drugs, their mechanisms of action, interactions, and targets.[13] We found 5 target proteins for the drug captopril using DrugBank, which may have implications in the treatment of various diseases.

Protein–protein interaction (PPI) network and signaling pathways of captopril DPTs analysis

STRING (search tool for the retrieval of interacting genes) resource is available online at https://string-db.org/ STRING database contains all known relationships between proteins, including both physical interactions and functional associations between them.[14] Therefore, we also used STRING database to identify multiple proteins associated with captopril, which are obtained from DrugBank. Initially, the search module was employed to find multiple proteins by their names ("DPTs") and the organism ("*Homo sapiens*"). Subsequently, the following settings were configured: the active interaction source was set to "Text mining and experimentation," the interaction score required was set to "Medium confidence (0.400)," the maximum number of interactions to display was set to "No more than 50 interactors," and the default options were used for all other settings. We also used this STRING database to identify the KEGG pathways of the target genes of captopril.[15]

To investigate the linkage between captopril and its associated genes in Bladder cancer (BLCA), we used 2 web-based tools: STITCH and NetworkAnalyst. STITCH (http://stitch.embl.de/) integrates data on metabolic pathway interactions and drug-target relationships to create a network that can be explored interactively or used as the foundation for more extensive studies.[16] Similarly, NetworkAnalyst (https://www.networkanalyst.ca/) is a comprehensive web-based application that allows bench researchers to perform standard and advanced meta-analyses of gene expression data via an intuitive web interface.[17,18] Thus, these 2 tools helped us to understand the interaction network between captopril and its associated genes in BLCA.

mRNA expression analysis of target genes BLCA

We utilized TNMplot (http://tnmplot.com/analysis/, accessed on September 28, 2023), a web tool for comparing DPTs gene expression between normal and tumor tissue in the bladder.[19] Mann Whitney was used for the statistical test between groups. UALCAN (http://ualcan.path.uab.edu) and GEPIA (http://gepia2.cancer-pku.cn/) web-based tools were also used to validate the expression results of DPT-related genes.

Survival analysis of target genes of captopril in BLCA

The online database Kaplan-Meier (available at https://kmplot.com/analysis/) was utilized to examine the relationship between target genes and the cumulative survival rates of

cancer patients. The analysis was conducted using data from the TCGA-BLCA cohort.[20] The patients were classified into 2 groups, high and low expression, according to the median level of captopril-associated gene's mRNA expression. Log-rank *P* values, hazard ratios, survival analysis plots, and 95% confidence intervals were analyzed in order to assess overall survival (OS) in BLCA patients. A total of 405 patients with BLCA were included in the study.

Identification of overexpressed genes in BLCA patients

GEO2R is a web tool that permits consumers to match 2 or more groups of samples in a GEO Series to find genes that are differentially expressed across experimental conditions. Using the GEO2R (https://www.ncbi.nlm.nih.gov/geo/geo2r/) online tool, we analyzed the differential gene expression between BLCA and normal samples.[21] The tool compared sample groups within a GEO Series (GSE65635) and examined gene symbols, where transcriptome analysis of normal and cancerous bladder tissues was performed. Malignant tumor samples were collected from patients after surgery, while noncancerous control samples were obtained from autopsies of healthy donors who died in road accidents. A pathologist examined both tumor and normal tissues to confirm the diagnosis and determine tumor cell counts. All tumor samples used in this study contained at least 80% tumor cells. To control false positives, adjusted P values were used together with the Benjamini and Hochberg false discovery rate method. The cutoff criteria were adjusted *P* value .05 and $|\log \text{Fold Change (FC)}| \leq 2$, ensuring that genes with significant differential expression in bladder cancer were identified.

Molecular docking

The wild type structures of the human proteins ACE, MMP9, and lipocalin 2 (LCN2) were retrieved from the AlphaFold Protein Structure Database (AlphaFold DB) using their UniProt accession codes I3UJJ7, P14780, and X6R8F3, respectively.[22] The wild MMP9 protein structure served as the template for generating the following mutated structures: F145L, C230W, H231P, S308F, and K566R, using the Swiss Model server.[23] Validation and energy minimization were achieved through the SAVES[24] and YASARA[25] webservers. Polar hydrogen atoms and Kollman charges were added prior to molecular docking using the AutoDock tools.

The structures of captopril, and other experimental/investigational drugs with similar chemical structures including epicaptopril, N-acetylproline, miridesap, and GPI-1485 were retrieved from the DrugBank database.[26] The PRODRG server was used for energy minimization.[27] Gasteiger charges were added using the AutoDock tools.

The CASTp server was used to predict the active binding pockets of ACE, MMP9, and LCN2.[28] The results were validated and were found consistent with the available information on the active site residues of these protein structures.[29,30] AutoDock Vina[31] was used for molecular docking of the drugs at the active binding pockets of the proteins, opting a grid-based docking protocol.[32] The Protein-Ligand Interaction Profiler (PLIP) webserver[33] was used to analyze the protein-ligand interactions.

Molecular dynamics simulations

Molecular dynamics (MD) simulations of the unbound proteins and the protein-ligand complexes were carried out using the GROMACS software (version 2019)[34] with GROMOS96 43a1 force field parameters.[35] The unbound proteins and the protein-ligand complexes were solvated using the TIP3P water model within a periodic boundary box of distance 1.0 nm.[36] Based on the rebalancing charges, the whole system was neutralized by adding an accurate concentration of Na+/Cl- ions.[37,38] Steepest descent method was used for energy minimization.[39] The thermostat coupling was set with a reference temperature of 300 K using the Berendsen thermostat,[39] and the pressure coupling was set with a reference pressure of 1 bar using the Parrinello-Rahman barostat.[39] The long-range interactions were estimated using the Particle-Mesh Ewald (PME) method.[40] The energy-minimized whole systems were equilibrated for 1000 ps at 300 K and 1 bar pressure in the NVT and NPT ensembles, respectively.[39,41] Molecular dynamics simulations were run for a timescale of 120 ns to understand the dynamic behavior and stability of the unbound proteins and the protein-ligand complexes. The root mean square deviations (RMSD) and the root mean square fluctuations (RMSF) of the unbound proteins and the protein-ligand complexes were estimated for MD simulation analysis. In addition, principal component analysis (PCA) was performed on the MD trajectories to explore the conformational motions and stability of the unbound proteins and the protein-ligand complexes.

Results

Identification of captopril's DPTs

Captopril is an ACE inhibitor as mentioned previously. It is described as extremely weak basic, cardiovascular agent, antihypertensive, renal protective agent, anti-inflammatory, antioxidant effect in output DB01197 from DrugBank 5.0. By using DrugBank, we identified 5 primary direct protein targets (DPTs) of captopril such as ACE, MMP2, MMP9, LTA4H, BDKRB1 (Table 1). The identification of DPTs can provide valuable insights into the specific pathways that may be modulated by captopril.

Captopril-regulated pathways in humans

In this study, the protein-protein interaction (PPI) network and signaling pathways associated with 5 DPTs of captopril

Table 1. Identification of direct targets of captopril using DrugBank.

PROTEIN TARGET	GENE	ACTIONS	ORGANISM
Angiotensin-converting enzyme	*ACE*	Inhibitor	Human
72 kDa type IV collagenase	*MMP2*	Inhibitor	Human
Matrix metalloproteinase-9	*MMP9*	Inhibitor	Human
Leukotriene A-4 hydrolase	*LTA4H*	Inhibitor	Human
B1 bradykinin receptor	*BDKRB1*	Not Available	Humans

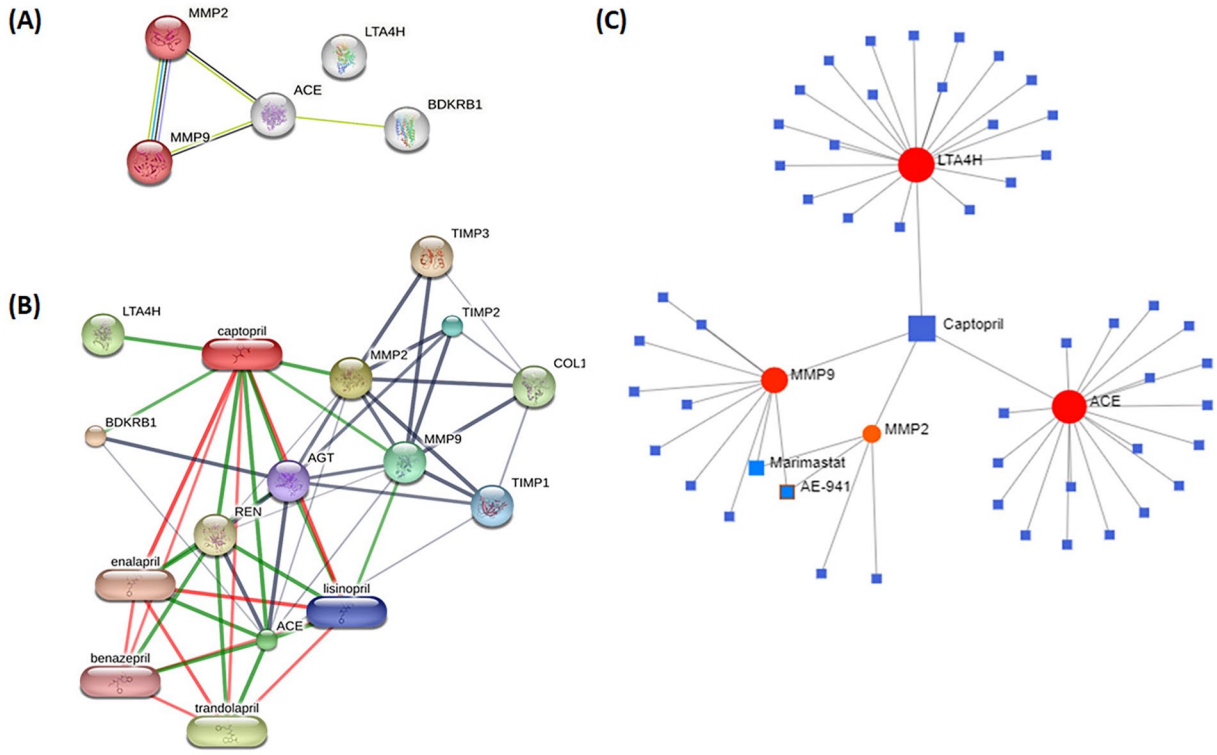

Figure 1. Relationship between captopril and captopril-associated genes. (A) Protein-protein interaction (PPI) network of captopril target genes (*ACE, MMP2, MMP9, BDKRB1, LTA4H*) from STRING. (B) STITCH and (C) NetworkAnalyst visualization of direct interactions between Captopril and LTA4H, ACE, MMP2, and MMP9.

were constructed using the STRING database (Figure 1A). Additionally, analyses using STITCH and NetworkAnalyst revealed direct interactions between captopril and specific proteins, namely LTA4H, ACE, MMP2, and MMP9 (Figure 1B and C). The visualizations generated by these tools provided valuable insights into the potential molecular associations that are relevant to the mechanism of action of captopril.

Moreover, the study identified the top 5 significant KEGG pathways associated with these DPTs, which include bladder cancer, endocrine resistance, leukocyte transendothelial migration, relaxin signaling pathway, fluid shear stress, and atherosclerosis (Table 2). Notably, bladder cancer (BLCA) was identified as the most relevant solid tumor linked to captopril, and 2 genes, *MMP2* and *MMP9*, were found to be involved in BLCA, supported by the STRING analysis.

mRNA expression profile of captopril associated genes in BLCA

In light of the substantial regulatory impact of Captopril on BLCA, we conducted an expression analysis of the genes associated with the direct target proteins DPTs that interact with Captopril specifically in BLCA. The findings are presented in Figure 2, which showcases the results obtained from the TNMplot web tool, focusing on *ACE*, *MMP2*, *MMP9*, *LTA4H*, and *BDKRB1* mRNA expression levels in both normal and tumor specimens of BLCA. Notably, it was observed that the expression of *MMP9* was significantly elevated in BLCA patients compared to normal samples (Figure 2C). This outcome was further supported by results obtained from ULCAN and GEPIA, as depicted in Supplemental Figures 1 and 2,

Table 2. List of KEGG pathway in captopril associated DPT.

PATHWAY	DESCRIPTION	COUNT IN NETWORK	STRENGTH	FALSE DISCOVERY RATE	GENE NAMES
hsa05219	Bladder cancer	2 of 41	2.38	0.0095	*MMP2, MMP9*
hsa01522	Endocrine resistance	3 of 517	1.45	0.0123	*MMP2, MMP9, BDKRB1*
hsa04670	Leukocyte transendothelial migration	2 of 95	2.01	0.0162	*MMP2, MMP9*
hsa04926	Relaxin signaling pathway	2 of 109	1.95	0.0162	*MMP2, MMP9*
hsa05418	Fluid shear stress and atherosclerosis	2 of 128	1.88	0.0175	*MMP2, MMP9*
hsa05205	Proteoglycans in cancer	2 of 133	1.87	0.0175	*MMP2, MMP9*
hsa05200	Pathways in cancer	2 of 196	1.7	0.0253	*MMP2, MMP9*

Abbreviations: MMP2, Matrix metallopeptidase 2;MMP9, Matrix metallopeptidase 9;BDKRB1, Bradykinin receptor B1

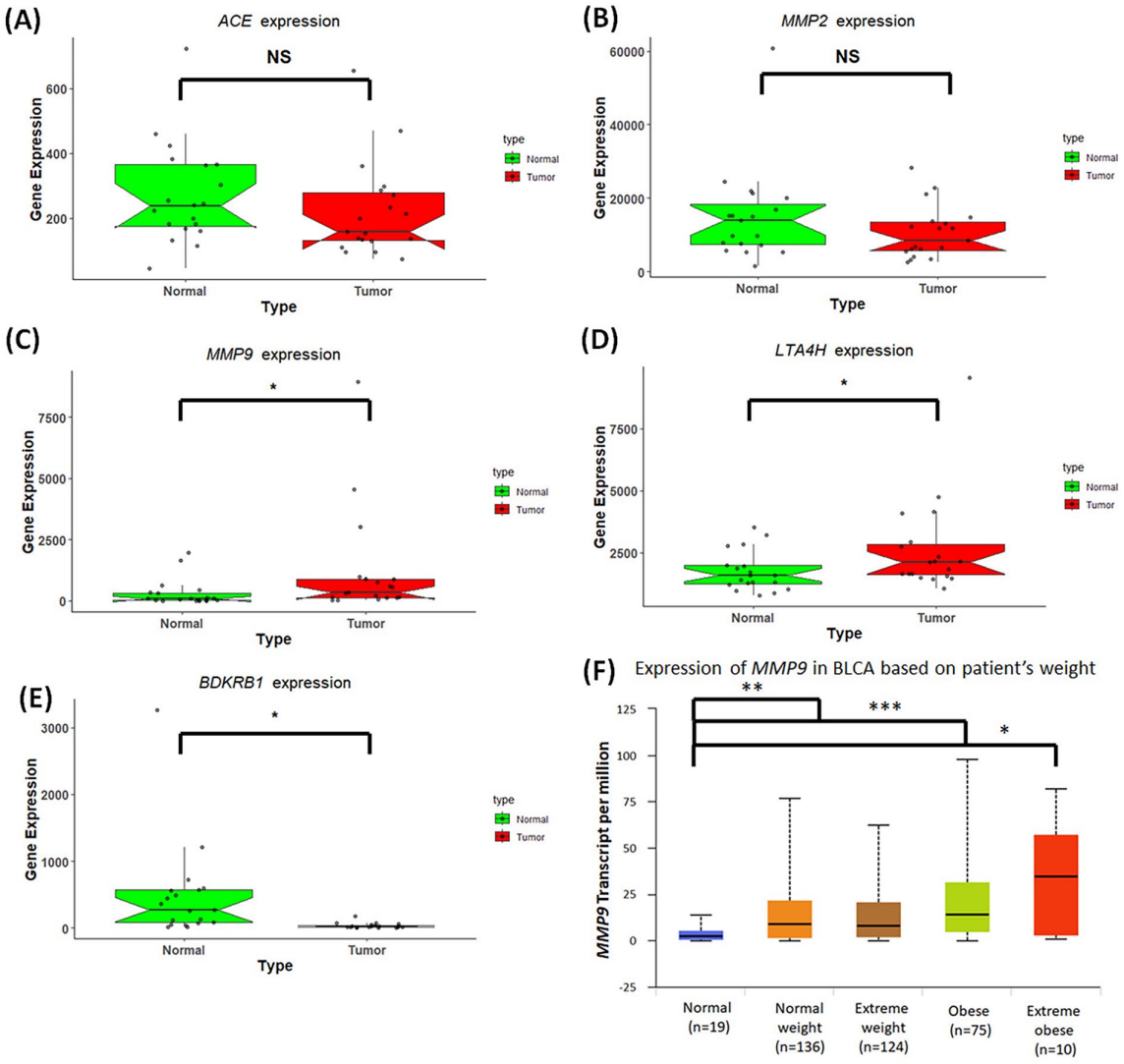

Figure 2. mRNA expression profile of captopril associated genes in BLCA. Box plot showing the expression of genes (A) *ACE* (B) *MMP2* (C) *MMP9* (D) *LTA4H* and (E) *BDKRB1*. RED color indicates bladder cancer and GREEN color means non-cancer/Normal. The X-axis of the plot shows normal and tumor samples and the Y-axis shows gene expression. The thick line in the middle represents the median, and the upper and lower limits of the box represent the third and first quartile respectively. Statistical analysis is Mann-Whitney *U* test (*P* values $<.05$=*, $<.005$=**, $<.0005$=***). (F) Expression (Transcript per million) of *MMP9* in Normal weight, Extreme weight, Obese and Extreme obese. Normal weight=BMI greater than equal to 18.5 and BMI less than 25; Extreme weight=BMI greater than equal to 25 and BMI less than 30; Obese=BMI greater than equal to 30 and BMI less than 40; Extreme obese=BMI greater than 40. Statistical analysis is Mann-Whitney *U* test (*P* values $<.05$=*, $<.005$=**, $<.0005$=***).

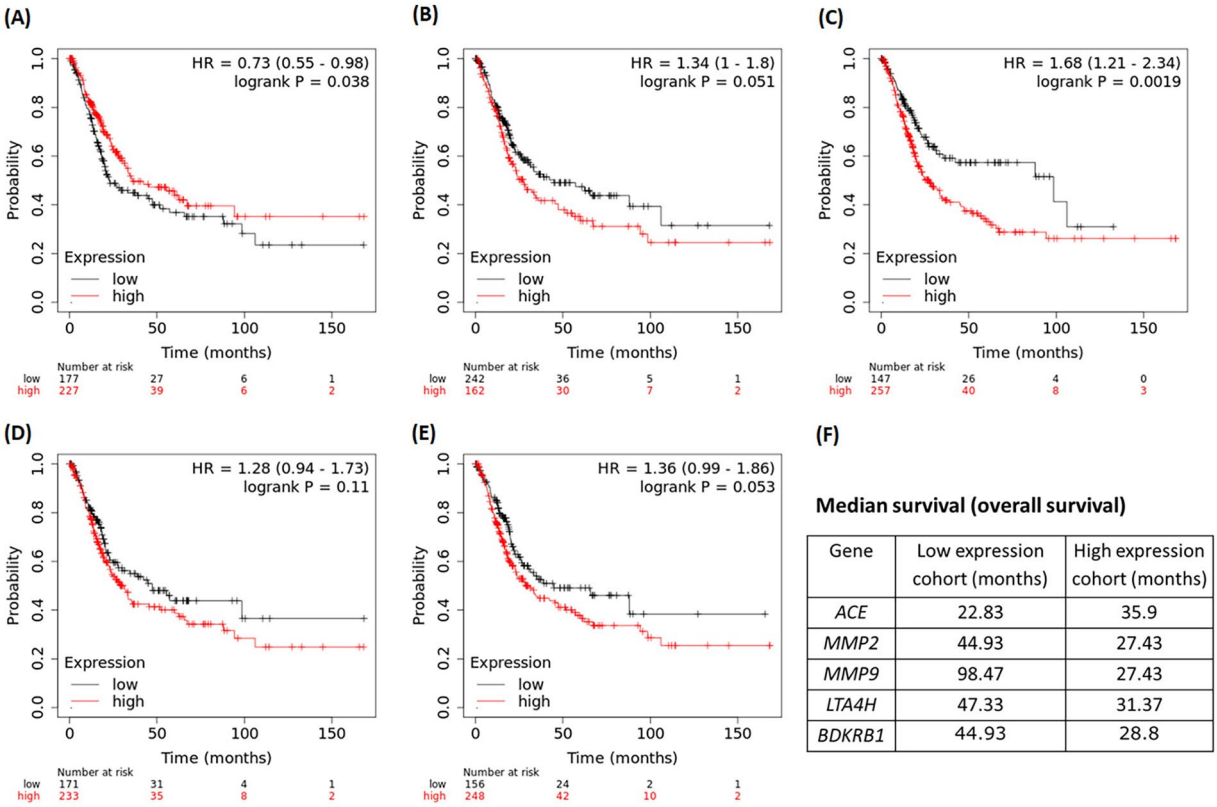

Gene	Low expression cohort (months)	High expression cohort (months)
ACE	22.83	35.9
MMP2	44.93	27.43
MMP9	98.47	27.43
LTA4H	47.33	31.37
BDKRB1	44.93	28.8

Figure 3. Association of captopril associated genes with overall survival in BLCA patients. Survival risk curves are shown for captopril DPT genes (A) *ACE* (B) *MMP2* (C) *MMP9* (D) *LTA4H* (E) *BDKRB1* expression in BLCA using KM-plotter. The expression ranges of the probes for *ACE*, *MMP2*, *MMP9*, *LTA4H*, and *BDKRB1* are 26-2345, 160-98392, 2-632587, 828-7249, and 1-1862, respectively. The cutoff values for these genes were 241, 8323, 207, 2195, and 22. Low and high expression level of genes are drawn in black and red respectively. *X*-axis shows per months or time and *Y*-axis shows probability of survival. In KM-plotter the threshold for the high and low gene expression cohorts is automatically calculated.

respectively. Additionally, through analysis using the ULCAN web tool, it was discovered that patients with extreme obesity, who are at a high risk of developing hypertension, exhibited heightened *MMP9* expression in BLCA (Figure 2F). Collectively, these results suggest a potential association between *MMP9* expression and BLCA, particularly in patients at a heightened risk for hypertension and severe obesity.

Identification of overall survival in BLCA based on gene expression

Subsequently, we assessed the relationship between the survival of BLCA patients and the expression levels of genes corresponding to the DPTs associated with captopril. Figure 3 depicts the overall survival (OS) rate of patients with BLCA based on the expression levels of *ACE, MMP2, MMP9, LTA4H*, and *BDKRB1*. Notably, the data shows that patients with high *MMP9* expression have a significantly lower overall survival rate than those with low expression (as shown in Figure 3C).

Common SNPs and structural alterations of MMP9 in BLCA

In order to assess the viability of targeting MMP9 with captopril in BLCA patients, a thorough analysis was carried out to identify all potential mutations within the MMP9 gene, focusing specifically on BLCA. Six single nucleotide polymorphisms (SNPs) in the *MMP9* gene were discovered using cBioportal data on BLCA, 3 of which are located in the protein's fibronectin type-II domain (H231P, C230W, and S308F) **(**Supplemental Table 1**)**. Further examination of these SNPs revealed no discernible differences in the percentage of disordered regions, alpha helix regions, beta strand regions, or transmembrane (TM) helix regions between the mutated and wild types (Supplemental Table 1).

Analysis of overexpressed genes in BLCA for evaluating the therapeutic benefits of captopril

We conducted an extensive analysis of captopril's DPTs and their associated proteins using the STRING database. Subsequently, we validated and visualized the interactions using Cytoscape, as depicted in Figure 4A. The PPI network of captopril DPTs was generated on STRING, applying a cutoff criterion that allowed for a maximum of 20 interactors in layers 1 and 2.

Furthermore, we identified overexpressed genes in bladder cancer (BLCA) by analyzing the GEO database (GSE656351) through GEO2R. Specifically, genes with adjusted *P*-values less than .05 and LogFC greater than 2 were considered significantly overexpressed in BLCA. We then utilized a Venn diagram to identify the common genes between captopril's

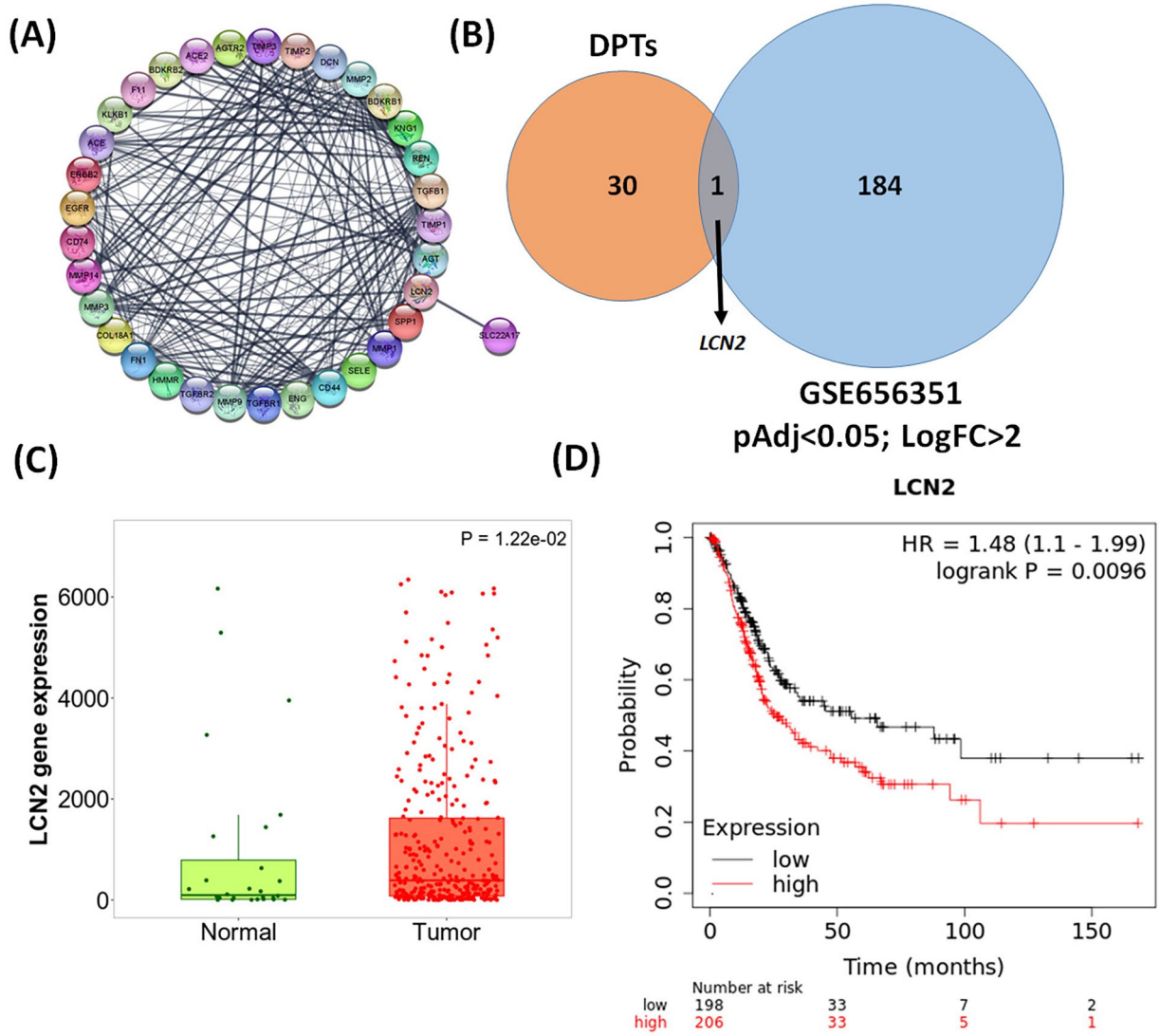

Figure 4. Identification of common DPTs of captopril and overexpressed genes in BLCA for assessing the benefits of captopril use. (A) Interaction of DPTs captopril with other proteins. (B) Common proteins between overexpressed genes in BCLA and interacting proteins with captopril DPTs. (C) Expression of *LCN2* gene in BLCA and normal tissue. ($P < .05$). (D) Survival risk curves are shown for *LCN2* expression in BLCA using KM-plotter. Expression range of the probe is 0 to 228 457 and cut-off is 707.
Abbreviations: DPTs, direct protein targets; BLCA, bladder cancer.

direct or indirect DPTs and the overexpressed gene in BLCA, as shown in Figure 4B. *LCN2* was the only one common gene.

The overexpression of *LCN2* in BLCA patients was further confirmed using the TNMPlot analysis, which demonstrated higher expression levels in paired tumor and adjacent normal tissues, as presented in Figure 4C. Notably, our findings revealed an intriguing association between the overexpression of *LCN2* and poor survival outcomes in BLCA patients, as illustrated in Figure 4D.

Interaction of captopril and similar experimental/investigational drugs with human ACE, MMP9, and LCN2

In the present study, we investigated the inhibitory prospects of captopril and other similar experimental/investigational drugs from DrugBank, including epicaptopril, N-acetylproline, miridesap, and GPI-1485 against the human proteins ACE, MMP9, and LCN2. Molecular docking of the drugs was performed at the active binding pockets of these proteins. The binding energy scores have been detailed in Table 3. It was evident from our analysis that captopril, a known inhibitor of human ACE[40] exhibited significantly higher ($P < .01$) binding potential with a binding energy score of -8.2 ± 0.03 kcal/mol, in comparison to the other similar experimental/investigational drugs (Table 3).

Captopril also produced the most promising binding energy score of -7.2 ± 0.01 kcal/mol with the human MMP9 protein, as compared to the other drugs (Table 3). Interaction profile (Figure 5A and B) revealed that captopril formed a hydrogen bond with Tyr423, a hydrophobic interaction with Pro421, a π-stacking with Tyr179 and a salt bridge with Lys603, at the active binding pocket of human MMP9. We also investigated the inhibitory potential of captopril against the mutated

Table 3. Binding energy scores (kcal/mol) of MMP9, LCN2 and ACE with captopril and similar drugs.

CAPTOPRIL AND SIMILAR EXPERIMENTAL DRUGS	PROTEINS		
	ACE	MMP9	LCN2
Captopril	−8.2 ± 0.03	−7.2 ± 0.01	−7.4 ± 0.02
DB02032	−7.7 ± 0.01	−6.7 ± 0.01	−6.8 ± 0.01
DB03360	−7.2 ± 0.01	−5.9 ± 0.03	−6.4 ± 0.02
DB05814	−7.4 ± 0.01	−6.2 ± 0.04	−6.1 ± 0.03
DB07384	−6.9 ± 0.03	−6.5 ± 0.01	−6.8 ± 0.03
DB07603	−6.8 ± 0.01	−5.8 ± 0.01	−6.9 ± 0.02
DB13087	−7.4 ± 0.01	−6.3 ± 0.02	−7.9 ± 0.02

Abbreviations: ACE, angiotensin-converting enzyme; MMP9, matrix Metallopeptidase 9; LCN2, Lipocalin 2.

MMP9 structures involving the mutations that are implicated in BLCA. Interestingly, captopril returned decent binding energy scores of −7.18 ± 0.02 kcal/mol, −7.20 ± 0.01 kcal/mol, −7.20 ± 0.01 kcal/mol, −7.19 ± 0.01 kcal/mol, and −7.20 ± 0.02 kcal/mol with the F145L, C230W, H231P, S308F, and K566R mutated structures of human MMP9, respectively (Supplemental Table 3).

Molecular docking revealed that the drug miridesap displayed the most encouraging binding energy score of −7.9 ± 0.02 kcal/mol with the human LCN2 protein, followed by captopril which produced a binding energy score of −7.4 ± 0.02 kcal/mol. Interaction profile of the captopril-LCN2 complex (Figure 5C and D) revealed that captopril formed hydrogen bonds with the amino acid residues Tyr106, Lys147, and Lys156, and hydrophobic interactions with the amino acid residues Tyr78 and Phe145, at the active pocket of human LCN2.

The investigational drug miridesap displayed a significantly higher ($P < .01$) binding energy score with LCN2 as compared to captopril. However, the binding energy scores were significantly lower ($P < .01$) for miridesap-ACE and miridesap-MMP9 complexes as compared to captopril-ACE and captopril-MMP9 complexes, respectively (Table 3). The aim of our study was to screen drugs that may show inhibitory potential against hypertension as well as BLCA. Captopril, the known inhibitor of ACE involved in hypertension, displayed encouraging binding energy scores with the human proteins MMP9 and LCN2, that are implicated in BLCA.[42,43] Accordingly, the captopril-MMP9 and captopril-LCN2 complexes were selected for further molecular dynamics simulations.

Analysis of molecular dynamics simulations

The unbound proteins MMP9 and LCN2, and the complexes of captopril with these proteins were subjected to molecular dynamics (MD) simulations for a timescale of 120 ns. The captopril-MMP9 and captopril-LCN2 complexes returned average RMSD values of 1.1 and 0.9 Å, respectively. The captopril-MMP9 and captopril-LCN2 complexes experienced initial fluctuations in RMSD values of Cα atoms and attained stability after 97 (Figure 6A) and 103 ns (Figure 6C), respectively, and remained stable thereafter. On the contrary, the unbound proteins MMP9 and LCN2 were found to display more fluctuations throughout the course of MD simulations displaying higher average RMSD values of 1.5 and 1.1 Å, respectively, than their corresponding captopril-bound complexes (Figure 6A and C). A low RMSD value is consistent with higher stability of a protein-ligand complex.[44]

RMSF analysis reveals the fluctuations in a protein–ligand complex during MD simulations and provides insights into conformational stability.[45] A thorough RMSF analysis of the unbound proteins MMP9 and LCN2, and their respective complexes with captopril revealed reduced fluctuations with lower average RMSF values among the complexes as compared to the unbound proteins (Figure 6B and D). The captopril-MMP9 and captopril-LCN2 complexes displayed average RMSF values of 1.2 and 1.4 Å, respectively (Figure 6B and D). However, the unbound proteins MMP9 and LCN2 produced average RMSF values of 1.6 and 1.8 Å, respectively. Interestingly, the residues at the active pockets of the proteins MMP9 and LCN2 that interacted with captopril suffered minimal fluctuations (Figure 6B and D). Our findings accentuate the conformational stability of the complexes.

Principal component analysis (PCA) was performed on the MD trajectories to explore the functional motions and conformational stability of the unbound proteins MMP9 and LCN2, and their complexes with captopril. The determination values were calculated from the atomic motions based on the eigenvectors. PCA analysis based on the principal components 1 and 2 (PC1 and PC2) have been depicted in Figure 7. It was evident from our analysis that the complexes of MMP9 and LCN2 with captopril (Figure 7B and D, respectively) were more compact in phase space in comparison to the unbound proteins MMP9 (Figure 7A) and LCN2 (Figure 7C). Compactness in phase space reflects narrow energy fluctuations and signifies higher stability.[39] PCA analysis reinforced the observation that binding of captopril to MMP9 and LCN2 imparted significant stability to the complexes.

Discussion

Captopril may be a good medication for a patient with bladder cancer (BLCA) who also has hypertension because it has many beneficial properties. This is especially important for BLCA patients who may be receiving chemotherapy or other treatments that might have negative cardiovascular side effects. Furthermore, captopril has been shown to have renal protective properties, which may help to prevent or delay the progression of kidney damage caused by BLCA or its treatment.[46] This is due to the presence of the primary direct protein target of

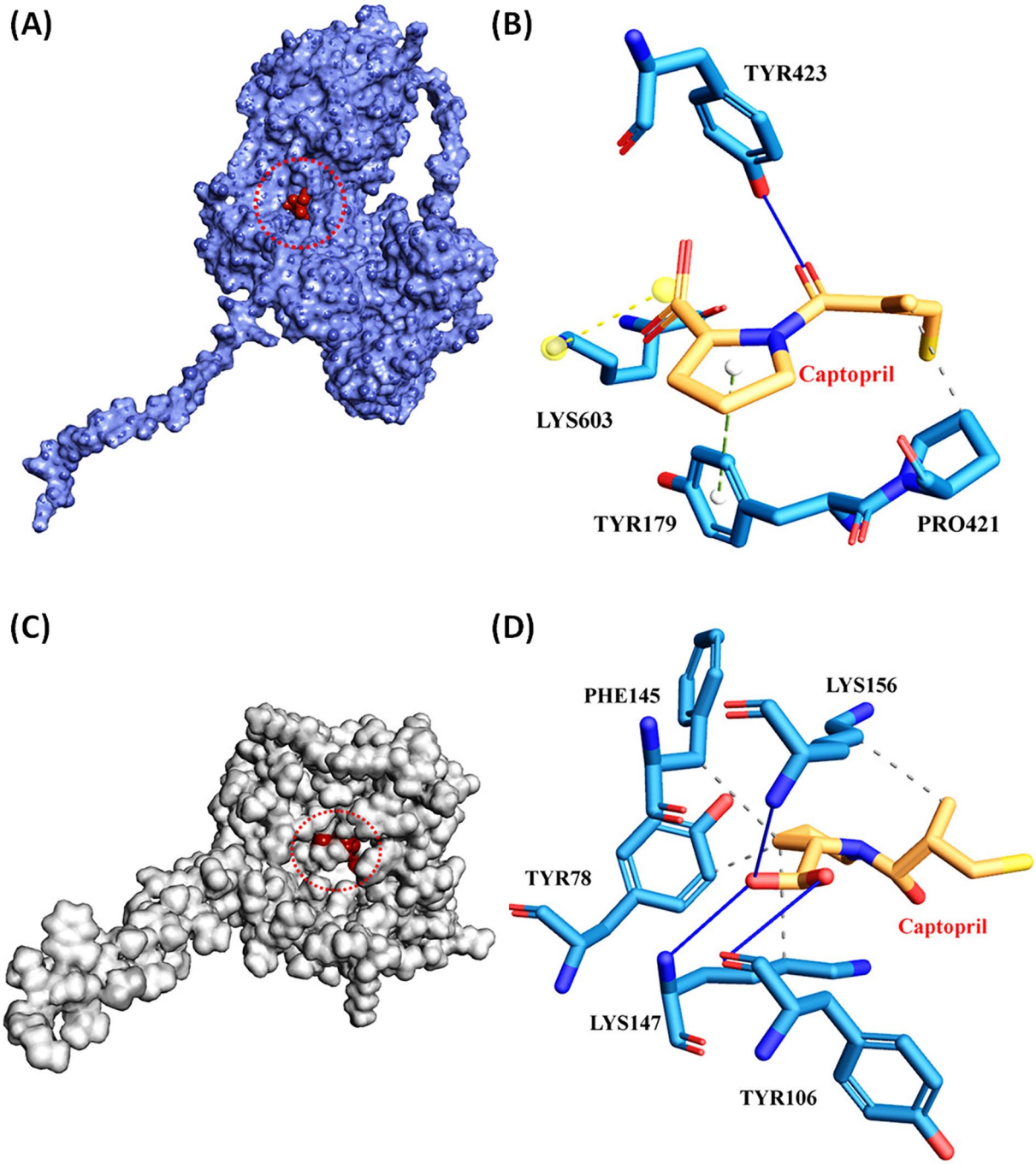

Figure 5. Interaction profile of captopril-MMP9 and captopril-LCN2 complexes. (A) Molecular docking of captopril with MMP9. Blue and brown spheres represent MMP9 and captopril, respectively. (B) Molecular interaction of captopril-MMP9 complex. Hydrophobic interactions are represented as gray dashed lines and hydrogen bonds are shown as blue lines. Green dashed lines show π-stacking interactions. Yellow dashed lines represent salt bridges. (C) Molecular docking of captopril with LCN2. Gray and brown spheres represent LCN2 and captopril, respectively. (D) Molecular interaction of captopril-LCN2 complex. Hydrophobic interactions and hydrogen bonds are represented as gray dashed lines and blue lines, respectively.

captopril, ACE, in the renin-angiotensin-aldosterone system, which regulates kidney and blood pressure.[46] Furthermore, it has been discovered that captopril's other 2 main direct protein targets, MMP2 and MMP9, are involved in a variety of BLCA-related processes such as leukocyte transendothelial migration, the relaxin signaling pathway, fluid shear stress, and atherosclerosis.[47] By blocking these targets, captopril might have additional anti-inflammatory and anti-cancer effects, which may be beneficial for BLCA patients. One study reported that captopril exhibits inhibitory effects on colon and prostate cancer cells. Captopril impedes cellular proliferation and cancer cell migration, potentially inducing apoptosis. These findings suggest that captopril could serve as an effective cancer therapeutic with reduced side effects.[10] Another study found that captopril, when combined with cyclophosphamide, enhanced the antitumor effects of cyclophosphamide in mice with Lewis lung

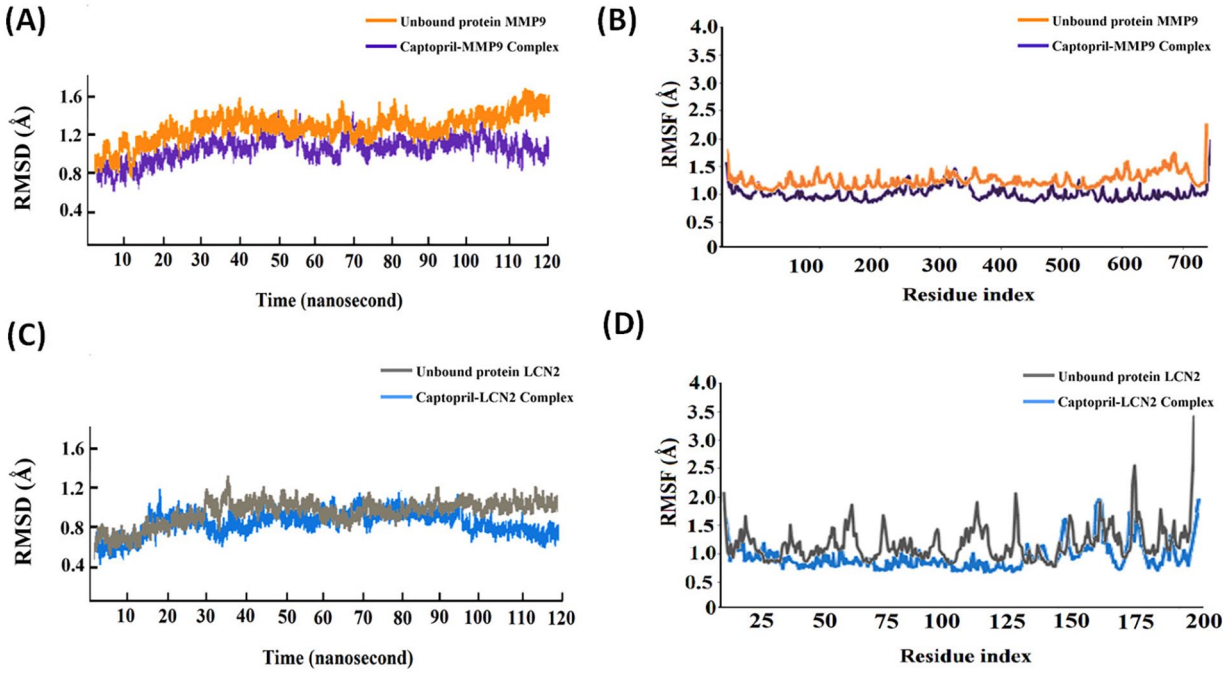

Figure 6. MD simulations of unbound protein MMP9, captopril-MMP9 complex, unbound protein LCN2, and captopril-LCN2 complex. (A) RMSD analysis of unbound MMP9 and captopril-MMP9 complex for 120 ns of MD simulations. (B) RMSF analysis of of unbound MMP9 and captopril-MMP9 complex for 120 ns of MD simulations. (C) RMSD analysis of unbound LCN2 and captopril-LCN2 complex for 120 ns of MD simulations. (D) RMSF analysis of unbound LCN2 and captopril-LCN2 complex for 120 ns of MD simulations.
Abbreviations: RMSD, root mean square deviation; RMSF, root mean square fluctuation.

carcinoma. However, administering captopril 5 days prior to cyclophosphamide treatment did not alter its antitumor activity. These findings indicate that captopril could be a potential treatment for cancer.[48]

Our study found that *MMP9* expression is significantly higher in BLCA, and high *MMP9* expression is linked to a lower overall patient survival. Furthermore, *MMP9* expression is increased in obese patients with BLCA who are at a higher risk of developing hypertension. MMP9 has been shown to promote tumor invasion by degrading the extracellular matrix and promoting tumor cell migration into nearby tissues.[49] MMP9 also activates inflammatory signaling pathways, promotes inflammatory cell migration to the arterial wall, and contributes to hypertension and other cardiovascular diseases.[50] As a result, measuring MMP9 levels in patients with hypertensive BLCA may aid in predicting prognosis and making treatment decisions. Overall, MMP9 is a key player in the progression of BLCA, particularly in obese-related hypertensive patients, and might be a promising target for the development of new diagnostic tools and therapies.

Our study also revealed the overexpression of *LCN2* in BLCA and its association with the protein targets affected by captopril. Furthermore, a separate study indicated an interaction among *LCN2, SLC22A17*, and *MMP9* genes, suggesting their cooperative role in cancer. Notably, the heightened expression of both *LNC2* and *MMP9* genes was observed in 16 tumor types, including BLCA, thus underscoring their involvement in tumor development.[51] High-molecular-weight matrix metalloproteinases (MMPs), like the LCN2-MMP-9 complex, have also been shown in studies to be independent predictors of metastatic phenotypes in a variety of cancers, including bladder and prostate cancer.[52] A recent study found that the LCN2/LOXL2/MMP9 ternary complex promotes cancer cell migration and invasion, as well as malignant tumor progression, making it a potential therapeutic target.[53] LCN2 and MMP9 form a complex, which protects MMP9 from degradation and thus increases its enzymatic activity.[54] This interaction is critical for modulating cancer cell metastatic behavior and is linked to the aggressive nature of neoplastic cells in a variety of cancers.[43] Thus, we proceeded to conduct further analysis to assess the ability of captopril and similar structures to inhibit MMP9 and LCN2.

Molecular docking analysis revealed promising inhibitory potential of captopril against human MMP9 protein. Captopril was found to interact with the Tyr179, Pro421, Tyr423, and Lys603 amino acid residues at the active pocket of MMP9. The catalytic domain residues Pro421 and Tyr423 of MMP9 have been reported to be instrumental in binding the reverse hydroxamate inhibitor through hydrogen bonds.[55] In addition, captopril displayed encouraging binding energy scores with the mutated MMP9 structures involving mutations that are implicated in BLCA.[56,57]

Captopril also returned promising binding energy score with the human LCN2 protein. It was found to interact with the Tyr78, Tyr106, Phe145, Lys147, and Lys156 residues at the active pocket of LCN2. Tyr78 and Tyr106 residues of LCN2 are imperative in ligand recognition and binding.[30] Our data from molecular docking were consistent with the results of

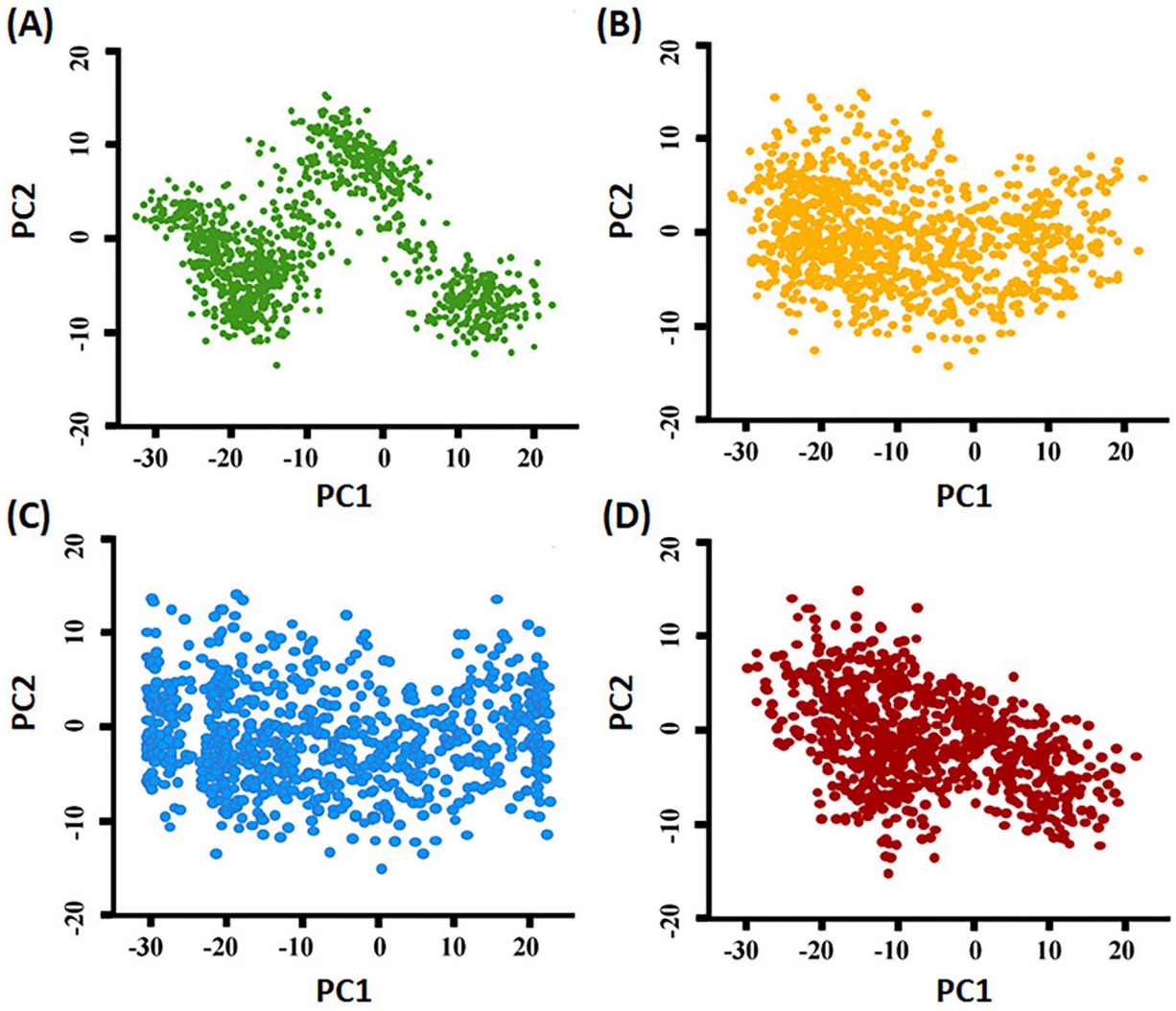

Figure 7. Principal component analysis (PCA) on the MD trajectories of unbound proteins and protein-ligand complexes in the phase spaces. (A) unbound protein MMP9. (B) captopril-MMP9 complex. (C) unbound protein LCN2. (D) captopril-LCN2 complex.
Abbreviation: PC, principal component.

MD simulations. The RMSD and RMSF trajectories for 120 ns of MD simulations revealed that the captopril-MMP9 and captopril-LCN2 complexes had more stable conformations in comparison to the unbound proteins MMP9 and LCN2. To further investigate the stability of the complexes, we compared their interaction profiles prior to and after MD simulations. The interaction profiles of the complexes after 120 ns of MD simulations have been provided as (Supplemental Figure 3). It was evident that the captopril-MMP9 (Figure 5B and Supplemental Figure 3A) and captopril-LCN2 (Figure 5D, Supplemental Figure 3B) complexes did not experience any change in interacting residues, following MD simulations.

Conclusion

Our comprehensive analysis reveals a significant association between the progression of bladder cancer BLCA and obesity-related comorbidities, with MMP9 emerging as a crucial mediator. These findings underscore the critical role of MMP9 in the development and progression of BLCA in the context of obesity, emphasizing the need to address these comorbidities for effective management and treatment of BLCA patients. Our findings also provide robust evidence of captopril's inhibitory potential against 2 critical human proteins, MMP9 and LCN2, which play a crucial role in BLCA. Remarkably, our results indicate that captopril exhibits equal efficacy in inhibiting both wildtype and mutated forms of MMP9, highlighting its broad applicability in treating BLCA patients with diverse genetic backgrounds. Nonetheless, further validation through in vitro and in vivo studies is imperative to consolidate and substantiate these promising findings. These investigations will facilitate the translation of captopril's therapeutic potential into clinical settings for the benefit of BLCA patients.

Authors' Note

Monisha Nandi is now affiliated to Department of Biomedical Science, College of Medicine, Kyung Hee University, Republic of Korea.

Acknowledgements
Not applicable

Author Contributions
All authors contributed to the study conception and design. Material preparation, data collection and analysis were performed by Sanjida Kabir Annana, Farzia Lamia, Ayan Roy, Jannatul Ferdoush, Pallab Kar, Monisha Nandi, Maliha Kabir and Ayan Saha. The first draft of the manuscript was written by Sanjida Kabir Annana and all authors commented on previous versions of the manuscript. Whole project was done under the supervision of Ayan Saha and Jannatul Ferdoush. All authors read and approved the final manuscript.

Availability of Data and Materials
Data are available from the corresponding author on reasonable request.

Ethics Approval and Consent to Participate
Not applicable

Consent for Publication
Not applicable.

ORCID iD
Ayan Saha https://orcid.org/0000-0003-1101-8372

Supplemental Material
Supplemental material for this article is available online.

REFERENCES
1. Zhou L, Xu J, Song Y, Gao Y, Chen X. Preparation and in vitro release performance of sustained-release captopril/chitosan-gelatin net-polymer microspheres. *J Ocean Univ China*. 2007;6:249-254.
2. Holman R, Turner R, Stratton I. Efficacy of atenolol and captopril in reducing risk of macrovascular and microvascular complications in type 2 diabetes: UKPDS 39. *Br Med J*. 1998;317:713-720.
3. Lewis EJ, Hunsicker LG, Bain RP, Rohde RD. The effect of angiotensin-converting-enzyme inhibition on diabetic nephropathy. *N Engl J Med*. 1993;329:1456-1462.
4. Volpert OV, Ward WF, Lingen MW, et al. Captopril inhibits angiogenesis and slows the growth of experimental tumors in rats. *J Clin Investig*. 1996;98:671-679.
5. Karagkouni D, Paraskevopoulou MD, Tastsoglou S, et al. DIANA-LncBase v3: indexing experimentally supported miRNA targets on non-coding transcripts. *Nucleic Acids Res*. 2020;48:D101-D110.
6. Kibret AA, Oumer M, Moges AM. Prevalence and associated factors of hemorrhoids among adult patients visiting the surgical outpatient department in the University of Gondar Comprehensive Specialized Hospital, Northwest Ethiopia. *PLoS One*. 2021;16:1-11.
7. Silva LB, de Oliveira DB, da Silva BV, et al. Identification and antifungal susceptibility of fungi isolated from dermatomycoses. *J Eur Acad Dermatol Venereol*. 2014;28:633-640.
8. Attoub S, Gaben AM, Al-Salam S, et al. Captopril as a potential inhibitor of lung tumor growth and metastasis. *Ann N Y Acad Sci*. 2008;1138:65-72.
9. Small W Jr, James JL, Moore TD, et al. Utility of the ACE inhibitor captopril in mitigating radiation-associated pulmonary toxicity in lung cancer: results from NRG Oncology RTOG 0123. *Am J Clin Oncol*. 2018;41:396-401.
10. Shebl RI. Anti-cancer potential of captopril and botulinum toxin type-A and associated p53 gene apototic stimulating activity. *Iran J Pharm Res*. 2019;18:1967-1977.
11. Ronquist G, Rodríguez LA, Ruigómez A, et al. Association between captopril, other antihypertensive drugs and risk of prostate cancer. *Prostate*. 2004;58:50-56.
12. Shirazi M, Soltani MR, Jahanabadi Z, et al. Stereological comparison of the effects of pentoxifylline, captopril, simvastatin, and tamoxifen on kidney and bladder structure after partial urethral obstruction in rats. *Korean J Urol*. 2014;55:756-763.
13. Wishart DS, Feunang YD, Guo AC, et al. DrugBank 5.0: a major update to the DrugBank database for 2018. *Nucleic Acids Res*. 2018;46:D1074-D1082.
14. Szklarczyk D, Gable AL, Nastou KC, et al. The STRING database in 2021: customizable protein-protein networks, and functional characterization of user-uploaded gene/measurement sets. *Nucleic Acids Res*. 2021;49:D605-D612.
15. Kanehisa M, Goto S. KEGG: Kyoto Encyclopedia of Genes and Genomes. *Nucleic Acids Res*. 2000;28:27-30.
16. Kuhn M, von Mering C, Campillos M, Jensen LJ, Bork P. STITCH: interaction networks of chemicals and proteins. *Nucleic Acids Res*. 2008;36:D684-D688.
17. Cerami E, Gao J, Dogrusoz U, et al. The cbio cancer genomics portal: an open platform for exploring multidimensional cancer genomics data. *Cancer Discov*. 2012;2:401-404.
18. Xia J, Gill EE, Hancock RE. NetworkAnalyst for statistical, visual and network-based meta-analysis of gene expression data. *Nat Protoc*. 2015;10:823-844.
19. Bartha Győrffy B. TNMplot.com: A web tool for the comparison of gene expression in normal, tumor and metastatic tissues. *Int J Mol Sci*. 2021;22:1-12. doi:10.3390/ijms22052622
20. Goel MK, Khanna P, Kishore J. Understanding survival analysis: Kaplan-Meier estimate. *Int J Ayurveda Res*. 2010;1:274-278.
21. Davis S, Meltzer PS. GEOquery: a bridge between the gene expression omnibus (GEO) and bioconductor. *Bioinformatics*. 2007;23:1846-1847.
22. Tunyasuvunakool K, Adler J, Wu Z, et al. Highly accurate protein structure prediction for the human proteome. *Nature*. 2021;596:590-596.
23. Waterhouse A, Bertoni M, Bienert S, et al. SWISS-MODEL: homology modelling of protein structures and complexes. *Nucleic Acids Res*. 2018;46:W296-W303.
24. Colovos C, Yeates TO. Verification of protein structures: patterns of nonbonded atomic interactions. *Protein Sci*. 1993;2:1511-1519.
25. Krieger E, Joo K, Lee J, et al. Improving physical realism, stereochemistry, and side-chain accuracy in homology modeling: four approaches that performed well in CASP8. *Proteins*. 2009;77(Suppl 9):114-122.
26. Wilczynski NL, McKibbon KA, Haynes RB. Sensitive clinical queries retrieved relevant systematic reviews as well as primary studies: an analytic survey. *J Clin Epidemiol*. 2011;64:1341-1349.
27. van Aalten DM, Bywater R, Findlay JB, et al. PRODRG, a program for generating molecular topologies and unique molecular descriptors from coordinates of small molecules. *J Comput Aided Mol Des*. 1996;10:255-262.
28. Tian W, Chen C, Lei X, Zhao J, Liang J. CASTp 3.0: computed atlas of surface topography of proteins. *Nucleic Acids Res*. 2018;46:W363-W367.
29. Kim HJ, Eichinger A, Skerra A. High-affinity recognition of lanthanide(III) chelate complexes by a reprogrammed human lipocalin 2. *J Am Chem Soc*. 2009;131:3565-3576.
30. Santiago-Sánchez GS, Noriega-Rivera R, Hernández-O'Farrill E, et al. Targeting Lipocalin-2 in inflammatory breast cancer cells with small interference RNA and small molecule inhibitors. *Int J Mol Sci*. 2021;22:1-19. doi:10.3390/ijms22168581
31. Trott O, Olson AJ. AutoDock Vina: improving the speed and accuracy of docking with a new scoring function, efficient optimization, and multithreading. *J Comput Chem*. 2010;31:455-461.
32. Kar P, Sharma NR, Singh B, Sen A, Roy A. Natural compounds fromclerodendrumspp. As possible therapeutic candidates against SARS-CoV-2: Anin silico-investigation. *J Biomol Struct Dyn*. 2021;39:4774-4785.
33. Salentin S, Schreiber S, Haupt VJ, Adasme MF, Schroeder M. PLIP: fully automated protein-ligand interaction profiler. *Nucleic Acids Res*. 2015;43:W443-W447.
34. Abraham MJ, Murtola T, Schulz R, et al. GROMACS: high performance molecular simulations through multi-level parallelism from laptops to supercomputers. *SoftwareX*. 2015;1-2:19-25.
35. Pol-Fachin L, Fernandes CL, Verli H. GROMOS96 43a1 performance on the characterization of glycoprotein conformational ensembles through molecular dynamics simulations. *Carbohydr Res*. 2009;344:491-500.
36. Bandaru S, Alvala M, Nayarisseri A, et al. Molecular dynamic simulations reveal suboptimal binding of salbutamol in T164I variant of β2 adrenergic receptor. *PLoS One*. 2017;12:1-22.
37. Patil SM, Phanindra B, Shirahatti PS, et al. Computational approaches to define poncirin from Magnolia champaka leaves as a novel multi-target inhibitor of SARS-CoV-2. *J Biomol Struct Dyn*. 2023;41:13078-13097.
38. Selvaraj C, Panwar U, Dinesh DC, et al. Microsecond MD simulation and multiple-conformation virtual screening to identify potential anti-COVID-19 inhibitors against SARS-CoV-2 main protease. *Front Chem*. 2020;8:1-15.
39. Chávez Thielemann H, Cardellini A, Fasano M, et al. From GROMACS to LAMMPS: GRO2LAM : a converter for molecular dynamics software. *J Mol Model*. 2019;25:147.

40. Odaka C, Mizuochi T. Angiotensin-converting enzyme inhibitor captopril prevents activation-induced apoptosis by interfering with T cell activation signals. *Clin Exp Immunol*. 2001;121:515-522.
41. Childers MC, Daggett V. Validating molecular dynamics simulations against experimental observables in light of underlying conformational ensembles. *J Phys Chem B*. 2018;122:6673-6689.
42. Tang YJ, Pang YH, Liu B. DeepIDP-2L: protein intrinsically disordered region prediction by combining convolutional attention network and hierarchical attention network. *Bioinformatics*. 2022;38:1252-1260.
43. Santiago-Sánchez GS, Pita-Grisanti V, Quiñones-Díaz B, et al. Biological functions and therapeutic potential of Lipocalin 2 in cancer. *Int J Mol Sci*. 2020;21:1-15. doi:10.3390/ijms21124365
44. Muralidharan N, Sakthivel R, Velmurugan D, Gromiha MM. Computational studies of drug repurposing and synergism of lopinavir, oseltamivir and ritonavir binding with SARS-CoV-2 protease against COVID-19. *J Biomol Struct Dyn*. 2021;39:2673-2678.
45. Kar P, Saleh-E-In MM, Jaishee N, et al. Computational profiling of natural compounds as promising inhibitors against the spike proteins of SARS-CoV-2 wild-type and the variants of concern, viral cell-entry process, and cytokine storm in COVID-19. *J Cell Biochem*. 2022;123:964-986.
46. Gan Z, Huang D, Jiang J, et al. Captopril alleviates hypertension-induced renal damage, inflammation, and NF-κB activation. *Braz J Med Biol Res*. 2018;51:1-9.
47. Xue WH, Li XW, Ding YQ, et al. Efficacy and safety of third-line or later-line targeted treatment for patients with metastatic colorectal cancer: a meta-analysis. *Front Oncol*. 2023;13:1-11.
48. Kowalski J, Herman ZS. Captopril augments antitumor activity of cyclophosphamide in mice. *Pol J Pharmacol*. 1996;48:281-285.
49. Augoff K, Hryniewicz-Jankowska A, Tabola R, Stach K. MMP9: A tough target for targeted therapy for cancer. *Cancers*. 2022;14:1-28. doi:10.3390/cancers14071847
50. Friese RS, Rao F, Khandrika S, et al. Matrix metalloproteinases: discrete elevations in essential hypertension and hypertensive end-stage renal disease. *Clin Exp Hypertens*. 2009;31:521-533.
51. Candido S, Tomasello B, Lavoro A, et al. Bioinformatic analysis of the LCN2-SLC22A17-MMP9 network in cancer: the role of DNA methylation in the modulation of tumor microenvironment. *Front Cell Dev Biol*. 2022;10:1-21.
52. Roy R, Louis G, Loughlin KR, et al. Tumor-specific urinary matrix metalloproteinase fingerprinting: identification of high molecular weight urinary matrix metalloproteinase species. *Clin Cancer Res*. 2008;14:6610-6617.
53. Xia Q, Du Z, Chen M, et al. A protein complex of LCN2, LOXL2 and MMP9 facilitates tumour metastasis in oesophageal cancer. *Mol Oncol*. 2023;17:2451-2471.
54. Yan L, Borregaard N, Kjeldsen L, Moses MA. The high molecular weight urinary matrix metalloproteinase (MMP) activity is a complex of gelatinase B/MMP-9 and neutrophil gelatinase-associated lipocalin (NGAL). Modulation of MMP-9 activity by NGAL. *J Biol Chem*. 2001;276:37258-37265.
55. Rowsell S, Hawtin P, Minshull CA, et al. Crystal structure of human MMP9 in complex with a reverse hydroxamate inhibitor. *J Mol Biol*. 2002;319:173-181.
56. Fouad H, Salem H, Ellakwa DE, Abdel-Hamid M. MMP-2 and MMP-9 as prognostic markers for the early detection of urinary bladder cancer. *J Biochem Mol Toxicol*. 2019;33:e22275.
57. Zeng Y, Gao M, Lin D, Du G, Cai Y. Prognostic and immunological roles of MMP-9 in pan-cancer. *Biomed Res Int*. 2022;2022:1-32.